ELSEVIER

Journal of Photochemistry and Photobiology A: Chemistry 112 (1998) 277–283

Journal of Photochemistry and Photobiology A:Chemistry

Photochemistry of acenaphthene at a silica gel/air interface

Celso Reyes [a], Michael E. Sigman [b,*], Rafael Arce [a,1], John T. Barbas [c], Reza Dabestani [b]

[a] *Department of Chemistry, University of Puerto Rico, Rio Piedras, PR 00931-3346, Puerto Rico*

[b] *Chemical and Analytical Sciences Division, Oak Ridge National Laboratory, PO Box 2008, MS 6100, Oak Ridge, TN 37831-6100, USA*

[c] *Department of Chemistry, Valdosta State University, Valdosta, GA 31698, USA*

Received 24 February 1997; received in revised form 26 May 1997; accepted 18 September 1997

Abstract

The photolysis of acenapthene (ACE) has been studied at a silica gel/air interface. Direct photolysis leads to 1-acenaphthenol as the principal photoproduct. Secondary photochemical conversion of the alcohol into 1-acenaphthenone is also observed. Reactions leading to formation of both 1-acenaphthenol and 1-acenaphthenone are attributed to electron-transfer oxidation mechanisms and the cation radical of ACE is directly observed by transient diffuse reflectance spectroscopy. Preconditioning the silica gel by heating at 200°C in air partially removes physisorbed water from the silica surface and photochemical conversion of ACE is observed to occur faster.

Keywords: Acenapthene; Photochemistry; Silica-gel/air interface

1. Introduction

Polycyclic aromatic hydrocarbons (PAH) are toxic, many are carcinogenic, and the widespread occurrence of these pollutants in the environment makes the photochemical oxidation of PAH a topic of current interest. Acenaphthene (ACE) is among the sixteen PAH singled out by the Environmental Protection Agency as priority pollutants [1]. ACE is reported to have a low vapor pressure (approximately 3 Pa at 25°C) and a sizable organic carbon sorption partition coefficient, log $K_{OC} \sim 4$ [2]. ACE has been estimated to react with singlet molecular oxygen at a rate $< 60\ M^{-1}\ s^{-1}$; [3] however, 1,8-dimethyl naphthalene, which is structurally very similar to ACE, is reported to react with singlet molecular oxygen at a rate of $2.7 \times 10^3\ M^{-1}\ s^{-1}$ [4]. When sorbed on different atmospheric particulate substrates, ACE has been determined to have photolytic half-lives of 2 h (silica gel), 2.2 h (alumina) and 44 h (fly ash) [5]. The observed effects of the substrates on the reported half-lives at the solid/air interfaces are unexplained for ACE, as for other PAH. A detailed mechanistic understanding of the photochemical reactions of a series of PAH on a number of substrates is required to understand the observed differences in photolytic half-lives. Previous work in our laboratories has focused on determining the photoproducts and mechanisms of the photochemical oxidation of PAH sorbed onto silicas and aluminas [6–15]. This study is a continuation of our efforts to understand PAH photochemistry under controlled conditions which allow for mechanistic interpretation and give insight into environmental processes.

Water-insoluble solid inorganic particles are found in the troposphere at concentrations estimated to be in the range of 1–300 mg m^{-3} [16]. Insulators such as SiO_2, Al_2O_3, silicoaluminates and $CaCO_3$ are thought to contribute up to 20–30% of inorganic atmospheric particulates [16]. The highly polar surfaces of inorganic oxide particulates found in the environment are simulated to a first approximation by commercial silicas and aluminas. Small PAH (anthracene and phenanthrene) in the lower troposphere have been shown to reside primarily in the gas phase at ambient temperatures. At upper tropospheric levels, where ambient temperatures are well below those at the earth's surface, even small PAH will reside sorbed on particulates and photochemical transformations at the particulate/gas interface can be expected to play a role in controlling the environmental fate of these pollutants [17].

2. Experimental

ACE (Aldrich Chemical, Milwaukee, WI; purity 99%) was recrystallized from ethanol twice before use. 1,8-

* Corresponding author. Tel.: +1-423-576-2173; fax: +1-423-574-4939; e-mail: sigmanme@ornl.gov

[1] Also corresponding author.

1010-6030/98/$19.00
PII S1010-6030(97)00290-6

Naphthalic anhydride (Aldrich; technical grade) 1,2-acenaphthenedione (Aldrich; technical grade) and acenaphthylene (Aldrich; purity 99%) were recrystallized from cyclohexane twice before use. 2,3-Naphthalenedicarboxaldehyde (Aldrich; reagent grade), 1-acenaphthenol (Aldrich; purity 99%) and 2,5-dimethylfuran (Aldrich; 99%) were used as received. 1-Acenaphthenone was prepared by oxidation of 1-acenaphthenol in acetone with dropwise addition of Jones reagent [18].

The physical characteristics of the SiO_2 (J.T. Baker, Phillipsburg, PA; reagent grade, 60–200 mesh) used in this work are identical to those previously reported [8]. The N_2 BET surface area for the SiO_2 was determined to be 274 $m^2\ g^{-1}$ with an average pore radius of 60 Å. The SiO_2 was used both unactivated and activated by heating for a minimum of 24 h at 200°C in air. The activated SiO_2 was cooled to room temperature in a desicator charged with anhydrous $CaSO_4$ prior to sorbing ACE. The SiO_2 was loaded with ACE (2.5×10^{-5} mol/g, 4.5% monolayer; 1.0×10^{-4} mol/g, 18% monolayer; and 5.0×10^{-4} mol/g, 90% monolayer) by adsorption from a cyclohexane (Baxter Healthcare, Burdick and Jackson Division, Muskegon, MI; HPLC grade) solution following the procedure outlined in earlier papers [6–15]. Photolysis was done in quartz tubes, irradiating with a 300 nm Rayonet photoreactor (irradiance of 2.68×10^{15} photons $cm^2\ s^{-1}$) and employing a horizontal tube orientation as previously described [6–15]. Photolysis was done under an atmosphere of air introduced directly into the tubes from the laboratory or under argon (Air Products, Knoxville, TN; ultra high purity) introduced after evacuation of the sample to 5 μm of mercury for 10 h. Photoproducts were removed by first washing the SiO_2 with methylene chloride and then with methanol. Products were analyzed by GC using an internal standard method with instrument responses determined from known materials. All products, except 1,8-naphthalenedicarboxaldehyde, were analyzed against materials of identical chemical structure obtained as detailed above. 1,8-Naphthalenedicarboxaldehyde was analyzed using commercially available 2,3-naphthalenedicarboxaldehyde as a standard.

Steady-state diffuse reflectance UV–visible spectra were recorded on a Cary-4 spectrophotometer equipped with an integrating sphere. Baseline correction was done with the spectrum recorded from a sample of SiO_2 that had not been loaded with organics. Diffuse Reflectance IR spectra were recorded on a Bio-Rad FTS-60 (Bio-Rad Laboratories, Digilab Division, Cambridge, MA) Fourier transform spectrophotometer. The spectrophotometer was calibrated and the baseline was recorded from a finely divided, oven-dried, KBr powder (Aldrich Chemical). The sample was prepared by mixing the SiO_2 with the KBr (1:3 respectively). Calibration as well as baseline and spectra measurements were performed after flushing the spectrometer sample chamber for 5 min with dry nitrogen. Emission spectra were recorded on a Spex Fluorolog fluorimeter and are reported fully corrected. Transient diffuse reflectance spectra were recorded after excitation with 266 nm light from a Quantel YG-660A NdYAG (Continuum, Santa Clara, CA) laser (4–10 mJ/pulse of 8 ns duration). The signal was collected using an apparatus previously described [19]. Transient absorption data are plotted as the difference in reflected intensity of a broad-band probe flash measured with and without laser excitation (ΔR) divided by the reflected intensity of the probe flash with no laser excitation (R).

3. Results

3.1. Photochemistry

Photolysis of ACE at a preconditioned silica gel/air interface (2.5×10^{-5} mol g^{-1} loading) leads to the generation of identifiable photoproducts 1-acenaphthenone (**1**), 1-acenaphthenol (**2**), 1,8-naphthalenedicarboxaldeheyde (**3**), acenaphthequinone (**4**), 1,8-naphthalic anhydride (**5**) and acenaphthylene (**6**). Product chemical structures are shown in Scheme 1 and the mole percent yield of each product, the mole percent of recovered ACE and the material balance are given in Table 1. The material balance remains fairly high (above 73%) through the first 6 h of photolysis. The largest single photoproduct is alcohol **2** (typically 64–68% of the products), and the second largest product is ketone **1** (typically 15–17% of the products). Traces of **6** (approximately 0.3–0.4 mole percent) are present in the starting material. Products **3**, **4**, and **5** are partly derived from singlet molecular oxygen mediated oxidation of **6**, as previously demonstrated [12]. The increased yield of **6** at longer photolysis times may result from dehydration of alcohol **2**. Direct photolysis of ACE was not stopped by the presence of co-sorbed 2,5-dimethyl furan (4.6×10^{-4} mol g^{-1}), a good singlet oxygen trap [20]. Likewise, the formation of **6** was not stopped by the presence of 2,5-dimethyl furan; however, the formation of **3**, **4** and **5** was inhibited. Direct photolysis of ACE at a lower surface coverage (2.5×10^{-6} mol g^{-1}) on preconditioned silica proceeded approximately five times faster than photolysis at the higher surface coverage; however, the prod-

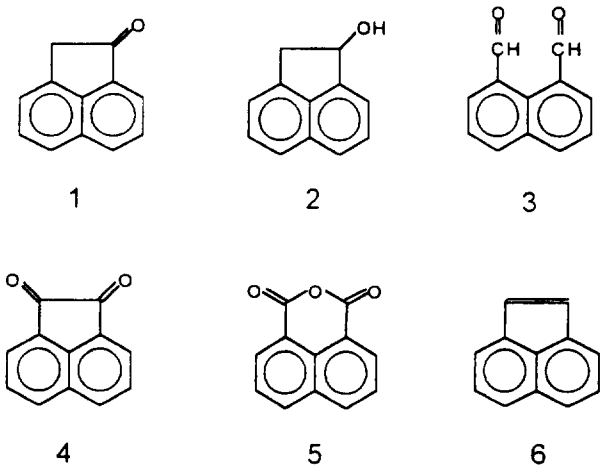

Scheme 1.

Table 1
Mole percent of products and remaining ACE as a function of photolysis time on silica preconditioned by heating at 200°C in air

	Photolysis time (h)					
	0.5	1	2	4	6	8
Acenaphthene (ACE)	83.1	80.2	70.6	56.6	50.9	38.2
Acenapthenone (1)	0.346	0.884	1.75	2.78	3.51	5.37
Acenaphthenol (2)	1.44	3.78	7.92	11.20	14.4	16.7
1,8-Naphthalene-dicarboxaldehyde (3)	0.166	0.618	1.38	2.23	3.33	3.65
Acenaphthequinone (4)						0.22
1,8-Naphthalic anhydride (5)						1.74
Acenaphthylene (6)	0.304	0.347	0.667	0.325	1.31	1.06
Total	85.356	85.829	82.317	73.135	73.45	66.94

Surface loading 2.5×10^{-5} mol g^{-1}.

uct distribution was essentially the same as observed at the higher coverage. This result is in agreement with our previous observations of surface coverage effects on PAH photochemistry at preconditioned silica gel/air interfaces [6–15].

Direct photolysis of ketone **1** (2.5×10^{-5} mol g^{-1}) sorbed on preconditioned silica resulted in no significant loss of the starting ketone over a photolysis period of 2 h. Photolysis of ketone **1** co-sorbed with ACE (2.5×10^{-5} mol g^{-1} each) yielded a similar result. Photolysis of alcohol **2** on preconditioned silica led to the formation of ketone **1**. Small amounts of **3**, **4** and **5** were formed from trace impurities of **6** present in the alcohol. Photolysis of alcohol **2** in the presence of co-sorbed 2,5-dimethylfuran also led to the formation of ketone **1**; however, the conversion of trace impurity **6** to give singlet molecular oxygen derived products **3–5** was stopped under the reaction conditions.

Photolysis of ACE on silica gel (2.5×10^{-5} mol g^{-1}) that had not been preconditioned by heating in air at 200°C proceeded approximately three times slower than photolysis at the same coverage on the preconditioned surface. Photolysis on the non-preconditioned surface gave a slight increased yield of alcohol **2** (76% of the products).

3.2. Steady-state spectroscopy

As the surface loading of ACE on preconditioned silica is increased from 1×10^{-5} mol g^{-1} to 5×10^{-4} mol g^{-1} there is a continuous change in the diffuse reflectance spectral profile, Fig. 1. As the surface coverage is increased, absorption on the red-edge of the spectrum is seen to increase and the maximum of the first band shifts to the red by 5 nm over the range of surface loadings investigated. Similarly, the fluorescence spectra of ACE on preconditioned silica gel (under an atmosphere of argon) are observed to undergo a change in spectral profile with increasing surface loadings from 1×10^{-5} mol g^{-1} to 5×10^{-4} mol/g, as shown in Fig. 2. The fluorescence spectra reveal two effects of increasing surface coverage: (1) a bleach on the blue-edge of the spectrum and (2) an increase in fluorescence intensity on the red-edge of the spectrum. Further insight into the nature of these spectral changes is given by the fluorescence and excitation spectra

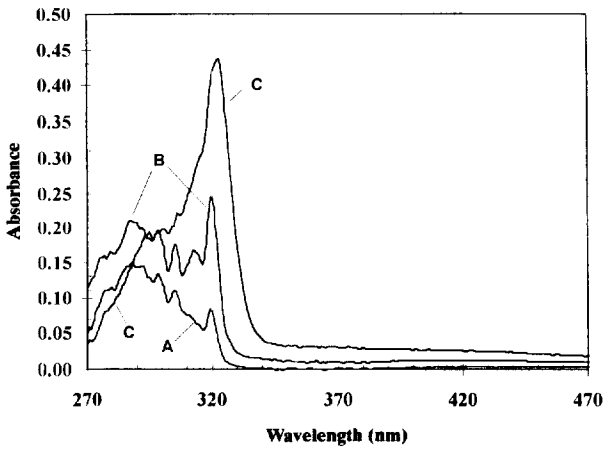

Fig. 1. Diffuse reflectance spectra of ACE on preconditioned silica at surface loadings of (A) 1×10^{-5} mol g^{-1} (B) 5×10^{-5} mol g^{-1} and (C) 5×10^{-4} mol g^{-1}.

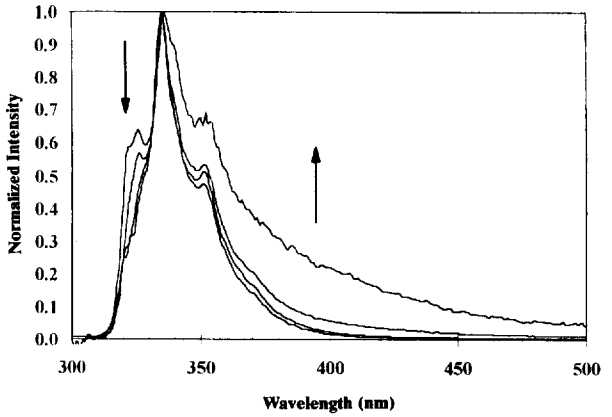

Fig. 2. Fluorescence spectra of ACE (under an atmosphere of argon) on preconditioned silica gel at surface loadings of 2.5×10^{-6} mol g^{-1}, 1×10^{-5} mol g^{-1}, 1×10^{-4} mol g^{-1} and 5×10^{-4} mol g^{-1}. The arrows in the figure show the direction of spectral change with increasing surface coverage.

shown in Fig. 3. All spectra in Fig. 3 were recorded at a surface loading of 5.0×10^{-4} mol g^{-1}. The fluorescence spectrum (Curve A; $\lambda_{ex}=288$ nm) is normalized at the 335 nm maximum. The excitation spectra (Curves B, C and D) were recorded by monitoring the emission at 335, 350 and

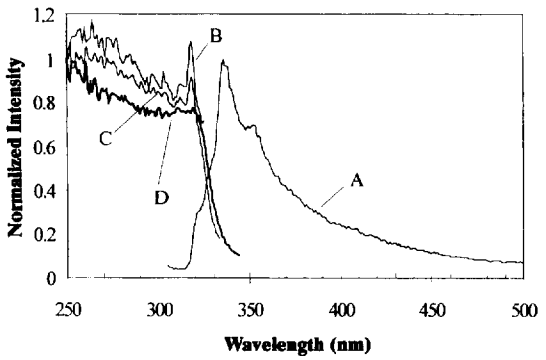

Fig. 3. Fluorescence spectrum (Curve A) of ACE (under an atmosphere of argon) on preconditioned silica gel at a surface loading of 5×10^{-4} mol g^{-1} ($\lambda_{ex} = 288$ nm) and excitation spectra (Curves B–D, $\lambda_{em} = 335$ nm, 350 nm and 390 nm respectively).

390 nm respectively. As the monitoring wavelength is moved to longer wavelength, the red-most band in the excitation spectrum is seen to reduce in intensity and a second species is observed under the ACE monomer profile. It is the formation of the new species that causes the increased absorption on the red edge of the diffuse reflectance absorption profile with increasing surface coverage, and the new species also corresponds to the increased intensity on the red edge of the fluorescence spectrum. The fluorescence of ACE on silica gel (surface loading of 1×10^{-5} mol g^{-1}) is 97% quenched under an atmosphere of air. Efficient fluorescence quenching of silica-sorbed PAH in air has previously been observed [6–15,21].

The new species that appears as the surface loading is increased is tentatively assigned to ground-state pairs, or higher aggregates, of ACE. An analogous change in the diffuse absorption spectral profile was previously observed for 1-methoxynaphthalene on silica gel at similar loadings [8]. The red-shift of the absorption spectrum at higher surface coverage is a phenomenon that we have observed on several occasions when studying the spectroscopy and photochemistry of PAH at silica gel/air interfaces [6–15]. The spectral assignment is further supported by the correspondence to the increased emission intensity observed on the red-edge of the fluorescence spectrum at higher surface coverage. The increased emission intensity is probably due to an excimer-like emission. Excimer emission has previously been reported from ACE in solution ($\lambda_{max} = 400$ nm) [22]. Excimer-like emission from ground-state associated pairs, and higher order aggregates, at silica-gel air interfaces is consistent with observations previously reported by ourselves, and others [6–15] [21]. The bleach on the blue edge of the fluorescence spectrum, observed with increasing surface loading, is likely due to reabsorption in the spectral region where the fluorescence and absorption overlap (an inner filter effect).

The normalized absorbance from the diffuse reflectance IR spectra of non-preconditioned (curve A) and preconditioned (curve B) samples of the SiO_2 used in this study are shown in Fig. 4. The spectral intensities of curves A and B have been normalized at 3749 cm^{-1}. The change in the spectra upon heating is due to partial loss of physisorbed water from the surface.

3.3. Time resolved spectroscopy

The transient diffuse reflectance spectrum for ACE at a preconditioned silica gel/argon interface (surface loading of 2.5×10^{-5} mol/g) is shown in Fig. 5 at 14, 26, 43 and 71 μs after laser excitation. Maxima are observed in the spectral profile at approximately 390, 440, 600 and 650 nm. The maximum is most intense in the first spectrum, recorded at 14 μs after laser excitation, and is seen to undergo a slight decay through 71 μs. Samples purged with O_2, show a similar spectral profile at 390, 600 and 650 nm; however the 440 nm peak is strongly quenched. We assign the transient at 390, 600 and 650 nm to the cation radical of ACE. The assignment is consistent with failure of O_2 to quench these bands, and is supported by previously reported absorption peaks at 388, 602 and 660 nm for the cation radical [23]. The band at 440 nm is assigned to the triplet–triplet absorption. This assign-

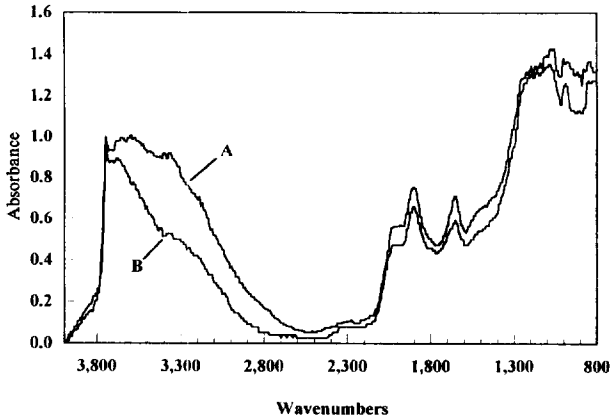

Fig. 4. Normalized absorbance from the diffuse reflectance IR spectra of (A) non-preconditioned and (B) preconditioned SiO_2 used in this study. The spectral intensities of curves A and B have been normalized at 3749 cm^{-1}.

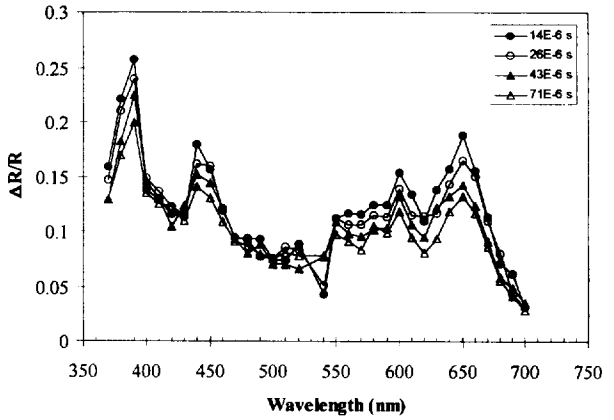

Fig. 5. Transient diffuse reflectance absorption spectrum for ACE at a preconditioned silica gel/air interface (surface loading of 2.5×10^{-5} mol g^{-1}).

ment is supported by oxygen quenching of the absorption and the previous assignment of the triplet–triplet absorption in solution at a wavelength of 433 nm in ethanol [24].

4. Discussion

Alcohol **2**, the major product formed in direct photolysis of ACE, comes from a pathway that is not mediated by singlet molecular oxygen. This conclusion is supported by the failure of 2,5-dimethylfuran to stop the reaction, as previously demonstrated for singlet oxygen mediated oxidation of other PAH at SiO_2/air interfaces [6–15]. Photochemical stability of ketone **1** (sorbed on silica by itself or co-sorbed with ACE) rules out formation of alcohol **2** by secondary photolysis of ketone **1**. Conversely, alcohol **2** is photochemically unstable on the silica surface and undergoes photolysis to give ketone **1** by a mechanism that is not singlet molecular oxygen mediated. On the basis of these observations, alcohol **2** is considered to be the initial photochemical product in the direct photolysis of ACE on silica and the origin of ketone **1** is assigned to the secondary photolysis of **2**. The observed photochemical stability of ketone **1** at the SiO_2/air interface may be attributed to slow migration by PAH on SiO_2 surfaces which prevents the triplet state of the ketone from abstracting hydrogen atoms from surface sorbed ACE. Additionally, efficient oxygen quenching of PAH excited singlet and triplet states at the silica/air interface, as demonstrated by the facile quenching of ACE fluorescence and triplet–triplet absorption, may also be responsible for the photochemical stability of the ketone.

Steady-state spectroscopic results provide evidence for a continuous increase in the formation of ground-state pairs (or higher aggregates) of ACE with increasing surface coverage on silica gel. Fluorescence spectroscopy reveals that ground-state pairs which lead to excimer-like emission are relatively low in concentration at ACE surface coverages less than 2.5×10^{-5} mol g^{-1}. Additionally, invariance in product distribution at 2.5×10^{-6} and 2.5×10^{-5} mol g^{-1} surface coverage demonstrates that ground-state pairs are not participating in the observed photochemistry. We are unaware of any reports of ACE photodimerization.

The observed photochemistry of ACE is consistent with a mechanism involving an electron transfer oxidation pathway. Data for other PAHs that are poor singlet molecular oxygen acceptors also supports an electron transfer photochemical oxidation pathway at SiO_2/air interfaces [9,10]. The transient spectroscopic data further supports this scenario and provides additional evidence for the formation of the cation radical of ACE upon excitation at the silica gel/air interface. A plot of cation radical $\Delta R/R$ intensity versus laser power would best determine if a monophotonic or biphotonic proc-

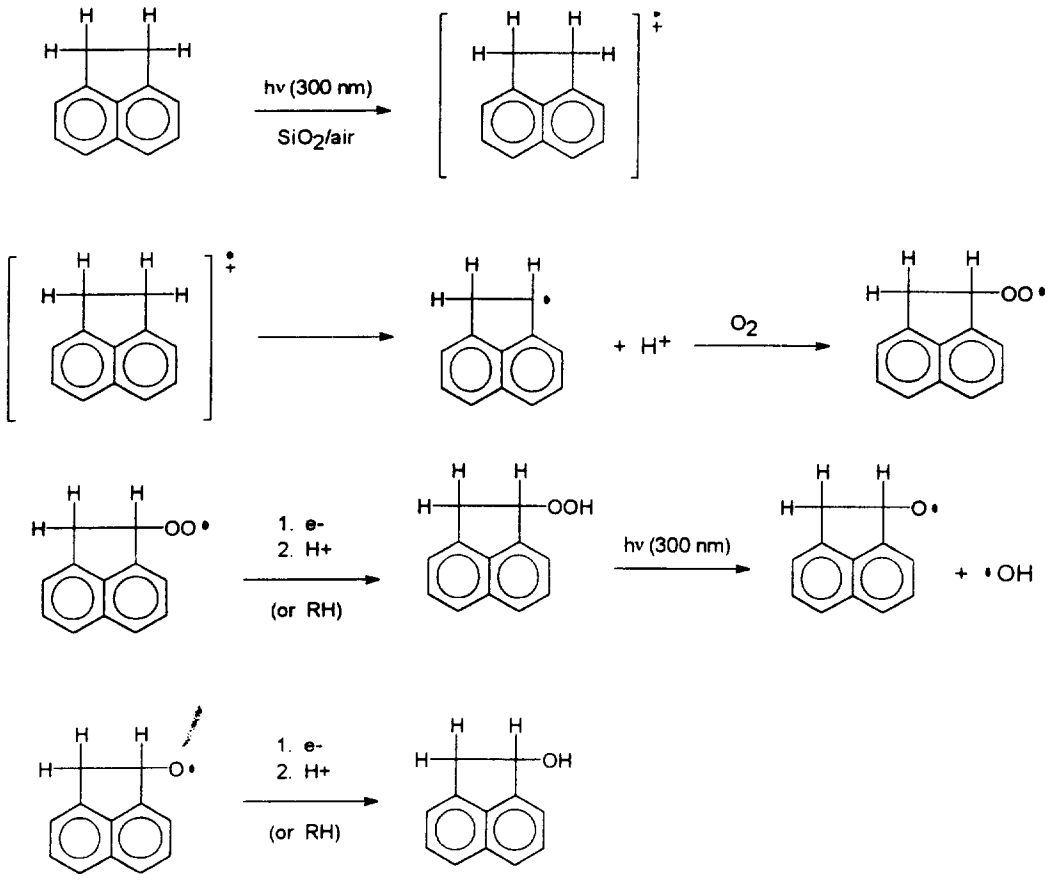

Scheme 2.

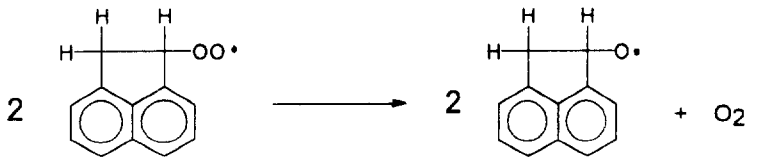

Scheme 3.

ess is responsible for the transient signal. Interpretation of the results of signal intensity versus laser power experiments is especially complicated, and often misleading, when dealing with weak signals as observed in the experiments described here [25]. Nonetheless, products attributable to electron-transfer processes, including superoxide, have previously been observed from the photolysis of naphthalene, 1-methylnaphthalene and 1-methoxynaphthalene at SiO_2/air interfaces with low intensity lamps [9,10]. The energy density in the conventional light sources used for our photoproduct studies is certainly too low to induce biphotonic processes, and a monophotonic oxidation mechanism which is not mediated by singlet molecular oxygen is required to explain the data. The data is consistent with the mechanism shown in Scheme 2. The mechanism in Scheme 2 may be augmented by the addition of a bimolecular step, shown in Scheme 3, a known reaction for solution phase oxidation; however, slow diffusion of surface-sorbed PAH and the observed invariance of product distribution at different surface loadings suggests that the bimolecular reaction in Scheme 3 does not play an important role in the observed photochemistry.

Surface sorbed water is observed to promote alcohol formation at the non-activated silica/air interface. This effect likely arises from slowing the secondary photochemistry which converts alcohol **2** into ketone **1**. The photochemical conversion of ACE to product is also slowed by the presence of water on the non-activated surface. The role of the surface-sorbed water in slowing these reactions may be to block surface 'active sites' by strong physisorption, thereby effectively reducing the ability of the surface to stabilize the highly polar intermediates formed during photochemical oxidation. Additional amounts of water could be removed from the surface by activation under more severe conditions, however, complete water removal would be accompanied by loss of silanol groups, leading to a dramatically different local environment for sorbed ACE [26]. These dramatic differences in the surface have been clearly demonstrated for naphthalene and pyrene sorbed on highly dehydrated silica [27]. The results presented here demonstrate a much more subtle effect observed at lower degrees of dehydration.

Acknowledgements

The authors gratefully acknowledge the assistance of Dr. Robert W. Redmond and his colleagues for providing assistance in collection of transient data at Wellman Laboratories of Photomedicine, Harvard Medical School, Massachusetts General Hospital. This research was sponsored by the Division of Chemical Sciences, Office of Basic Energy Sciences, US Department of Energy under contract DE-AC05-96OR22464 with Oak Ridge National Laboratory, managed by Lockheed Martin Energy Research and by a US DOE/EPSCoR grant DE-FGO2-94ER-75764 to the University of Puerto Rico.

References

[1] M.A. Callahan, M.W. Slimak, N.W. Gabelc, I.P. May, C.F. Fowler, J.R. Freed, P. Jennings, R.L. Durfee, F.C. Whitmore, B. Maestri, W.R. Mabey, B.R. Holt, C. Gould, US Environmental Protection Agency, Washington, DC, (1979), EPA-440/4-79-029.
[2] D. Mackay, W.Y. Shiu, K.C. Ma, Illustrated Handbook of Physical–Chemical Properties and Environmental Fate for Organic Chemicals, Vol. II, Lewis Publishers, Chelsea, MI, (1992) pp. 117–121.
[3] W. Mabey, J.H. Smith, R.T. Podoll, H.L. Johnson, T. Mill, T.W. Chou, J. Gate, I. Waight-Partridge, H. Jaber, D. Vandenberg, US Environmental Protection Agency (1982), EPA-440/4-81-14.
[4] C.J.M. van den Heuvel, H. Steinberg, T. de Boer, J. Recueil, J. R. Neth. Chem. Soc. 99 (1980) 109.
[5] T.D. Behymer, R.A. Hitse, Environ. Sci. Technol. 19 (1985) 1004.
[6] R. Dabestani, K.J. Ellis, M.E. Sigman, J. Photochem. Photobiol. A: Chem. 86 (1995) 231.
[7] M.E. Sigman, E.A. Chevis, A. Brown, J.T. Barbas, R. Dabestani, E.L. Burch, J. Photochem. Photobiol. A: Chem. 94 (1996) 149.
[8] M.E. Sigman, J.T. Barbas, E.A. Chevis, R. Dabestani, New J. Chem. 20 (1996) 243.
[9] R. Dabestani, M. Nelson, M.E. Sigman, J. Photochem. Photobiol. 64 (1996) 80.
[10] J.T. Barbas, R. Dabestani, M.E. Sigman, J. Photochem. Photobiol. A: Chem. 80 (1994) 103.
[11] M.E. Sigman, S.P. Zingg, in: D. Helz, R.G. Zepp (Eds.), Environmental Aspects of Surface and Aquatic Photochemistry, Lewis Publishers, Boca Raton, FL (1994) p. 197.
[12] S.P. Zingg, M.E. Sigman, Photochem. Photobiol. 57 (1993) 453.
[13] J.T. Barbas, M.E. Sigman, A.C. III Buchanan, E.A. Chevis, Photochem. Photobiol. 58 (1993) 155.
[14] S.P. Zingg, R.M. Pagni, J.H. Burns, M.E. Sigman, Tetrahedron Lett. 32 (1991) 5737.
[15] J.T. Barbas, M.E. Sigman, R. Dabestani, Environ. Sci. Technol. 30 (1996) 1776.
[16] C. Guillard, H. Delprat, C. Hoang-van, P. Pichat, J. Atmos. Chem. 126 (1993) 47 and references cited therein .
[17] H. Yamasaki, K. Kuwata, H. Miyamoto, Environ. Sci. Technol. 16 (1982) 189.
[18] L.F. Fieser, M. Fieser, Reagents for Organic Synthesis, Vol. 1, Wiley, New York (1967) p. 142.
[19] B. Avehno, T. Hagan, R.W. Redmond, Photochem. Photobiol. 59 (1994) 328.
[20] K. Gollnick, A. Griesbeck, Photochem. Photobiol. 41 (1985) 2057.
[21] J.K. Thomas, Chem. Rev. 93 (1993) 301 and references cited therein .
[22] J.B. Birks, Photophysics of Aromatic Molecules, Wiley-Intersience, New York (1970) pp. 301–371.

[23] T. Shida, Electronic Absorption Spectra of Radical Ions, Elsevier, New York (1990) pp. 65–66.
[24] I. Carmichael, G.L. Hug, J. Phys. Chem. Ref. Data 15 (1986) 1.
[25] U. Lachish, A. Shafferman, G. Stein, J. Chem. Phys. 64 (1976) 4205.
[26] R.K. Iler, The Chemistry of Silica: Solubility, Polymerization, Colloid and Surface Properties and Biochemistry, Wiley, New York, 1979.
[27] R.K. Bauer, P. DeMayo, L.V. Natarajan, W.R. Ware, Can. J. Chem. 62 (1984) 1279.